Earth and Space Science

RESEARCH LETTER
10.1029/2020EA001253

Comprehensive High-Precision Relocation of Seismicity on the Island of Hawai'i 1986–2018

Robin S. Matoza[1], Paul G. Okubo[2], and Peter M. Shearer[3]

[1]Department of Earth Science and Earth Research Institute, University of California, Santa Barbara, CA, USA, [2]Department of Earth Sciences, University of Hawai'i at Manoa, Honolulu, HI, USA, [3]Institute of Geophysics and Planetary Physics, Scripps Institution of Oceanography, University of California, San Diego, CA, USA

Key Points:

- We present a new catalog of high-precision relocated seismicity across the Island of Hawai'i from 1986 to 2018
- Dramatic sharpening of seismicity along faults, streaks, rings, rift zones, magma pathways, and mantle fault zones
- Relocated catalog captures almost the entire 1983–2018 Pu'u 'Ō'ō-Kūpaianaha eruption of Kīlauea

Supporting Information:

- Supporting Information S1
- Supporting Information S2
- Dataset S1
- Movie S1
- Movie S2
- Movie S3

Correspondence to:
R. S. Matoza,
rmatoza@ucsb.edu

Citation:
Matoza, R. S., Okubo, P. G., & Shearer, P. M. (2020). Comprehensive high-precision relocation of seismicity on the Island of Hawai'i 1986–2018. *Earth and Space Science*, *7*, e2020EA001253. https://doi.org/10.1029/2020EA001253

Received 30 APR 2020
Accepted 24 OCT 2020

Abstract Abundant seismicity beneath the Island of Hawai'i from mantle depths to the surface plays a central role in understanding how volcanoes work, grow, and evolve at this intraplate oceanic hotspot. We perform systematic waveform cross-correlation, cluster analysis, and relative relocation of 347,445 events representing 32 years of seismicity on and around the island from 1986 to 2018. We successfully relocate 275,009 (79%) events using ~1.7 billion differential times (*P* and *S*) from ~128 million similar-event pairs. The results reveal a dramatic sharpening of seismicity along faults, streaks, rings, rift zones, magma pathways, and mantle fault zones; seismicity delineating crustal detachments on the flanks of Kīlauea and Mauna Loa is particularly well-resolved. The resulting high-precision spatio-temporal image of seismicity captures almost the entire 1983–2018 Pu'u 'Ō'ō-Kūpaianaha eruption of Kīlauea with its numerous distinct episodes and wide-ranging activity, culminating in the 2018 lower East Rift Zone eruption and summit collapse.

Plain Language Summary We present a new catalog of high-precision relocated seismicity across the Island of Hawai'i from 1986 to 2018, a location that has long served as a natural laboratory for studying magmatic and tectonic processes.

1. Introduction

The Island of Hawai'i is one of the most volcanically and seismically active regions on Earth, with all seismicity in this intraplate setting ultimately resulting directly or indirectly from volcanism (Eaton, 1962). Seismicity recorded on the island is principally concentrated around and beneath the active summits and rift zones of the basaltic shield volcanoes Kīlauea and Mauna Loa and Lō'ihi seamount offshore (Figures 1 and 2). Dense seismicity occurs beneath mobile flanks and fault systems of these volcanoes, accommodating stress from repeated intrusions and gravitational instability from volcano growth (e.g., Brooks et al., 2006; Got & Okubo, 2003; Got et al., 1994; Owen et al., 1995; Segall et al., 2006; Swanson et al., 1976). Additional deeper earthquakes around the island (e.g., the 2006 *Mw* 6.7 Kīholo Bay earthquake) have been attributed to lithospheric flexure and subsidence of the entire island due to volcano loading, with additional stresses of magmatic origin probably contributing at shallower depths (e.g., Klein et al., 1987; Wolfe et al., 2004, 2003; Yamada et al., 2010). Deeper (>13 km) seismicity in some regions is concentrated along low-angle planes interpreted as preexisting fault zones in the lower crust and upper mantle (Wolfe et al., 2003, 2004). Large damaging earthquakes (*Mw* 6–8) regularly occur and represent a tsunami hazard (Klein et al., 2001). The high seismicity rates in conjunction with time-dependent variations in volcanism and geodetically observed deformation have established the Island of Hawai'i as a natural laboratory for elucidating interactions between magmatic and tectonic processes (e.g., Eaton & Murata, 1960; Klein et al., 1987; Poland, 2015; Ryan, 1988; Swanson et al., 1976; Tilling & Dvorak, 1993).

Instrumental seismic observations began on the Island of Hawai'i over a century ago (Jaggar, 1920). A permanent telemetered electronic seismic network was first installed by HVO in the late 1950s (Eaton & Murata, 1960) and has steadily expanded ever since. Digital event-triggered waveform data from the network become available from 1986 starting with the Caltech-USGS Seismic Processing (CUSP) system, transitioning in 2009 to the AQMS system (AQMS: ANSS Quake Management System; ANSS: Advanced National Seismic System) (Figure 1).

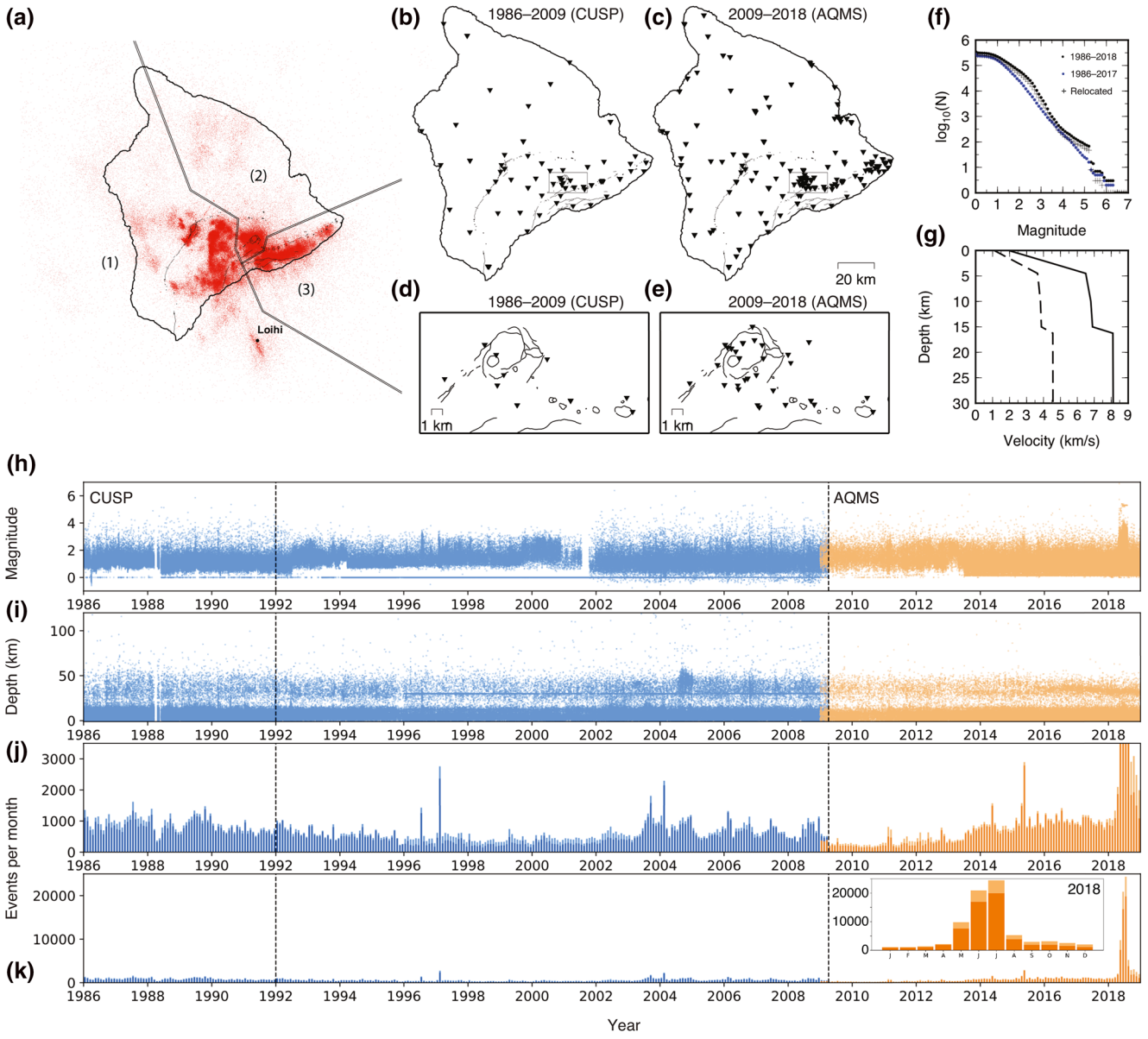

Figure 1. Data and inputs used in this study. (a) Starting catalog locations for all seismicity on the Island of Hawai'i 1986–2018. To reduce memory requirements, we divide the seismicity into three polygons ([1], [2], [3]) along natural breaks in seismicity, which we process separately. (b–e) HVO seismic network and additional stations on the Island of Hawai'i for which event-based waveform data are available from (b and d) the CUSP system (1986–2009; 144 channels) and (c and e) the AQMS system (2009–2018; 565 channels). (f) Gutenberg-Richter (G-R) magnitude-frequency relations; *N* is the number of events with magnitude greater than or equal to magnitude *M*. Deviation from a G-R law coincides with the unusual seismicity occurring at Kīlauea in 2018. (g) The 1-D velocity model (Klein, 1981) used in this study. (h–k) Catalog evolution for the (blue) CUSP 1986–2009 and (orange) AQMS 2009–2018 events considered in this study. (h) Local magnitude, (i) depth (km), (j) number of events per month, (k) number of events per month with expanded scale to show 2018 (max 24,350 events per month). In (j) and (k), darker shading indicates relocated seismicity. ANSS, Advanced National Seismic System; AQMS, ANSS Quake Management System; CUSP, Caltech-USGS Seismic Processing; HVO, Hawaiian Volcano Observatory.

Here we present a new comprehensive high-precision catalog of relocated hypocenters representing 32 years of seismicity on and around the Island of Hawai'i from 1986 to 2018, produced through systematic reanalysis of the available event-based digital waveform data.

2. Data and Methodology

Dramatic improvements in relative earthquake locations among nearby events can be achieved by exploiting the fact that the biasing effects of 3-D structure are similar for closely spaced events (e.g., Shearer et al, 2005; Waldhauser & Ellsworth, 2000). Here we perform systematic waveform cross-correlation and attempt relative relocation for all seismicity on the Island of Hawai'i from 1986 to 2018 recorded by the permanent telemetered HVO network and additional stations integrated in HVO operations (Figure 1). We use the 1-D velocity model of Klein (1981) (Figure 1g) and aim to improve relative earthquake precision within similar event clusters without shifting absolute earthquake locations (cluster centroids) or solving for a 3-D velocity model.

2.1. Seismic Waveform Data and Starting Hypocenter Catalog

We start with digital event-based waveform data for all seismicity cataloged by HVO, including both automatic event triggers (no analyst phase-pick data) and interactively located events (with analyst phase-pick data). The starting catalog locations are produced using the 1-D velocity model of Klein (1981) (Figure 1g) (e.g., Nakata & Okubo, 2010). We first merge seismic waveform data and metadata from separate CUSP (1986–2009; 144 channels) and AQMS (2009–2018; 565 channels) acquisition systems, representing increasingly expansive network coverage (Figures 1b–1e). Station coverage is particularly enhanced in the Kīlauea summit region with the AQMS data through integration of the permanent broadband seismic network (Dawson et al., 1998). Seismic instrumentation also improved over time, with short-period vertical-component instruments typical of the CUSP data gradually being replaced by more three-component broadband instruments. We merge these datasets and metadata, converting them to a common, custom, event-based format (termed EFS for "Event Filing System"), greatly facilitating systematic analyses.

A previous study by Matoza et al. (2013) considered 130,902 seismic events from January 1992 to March 2009 acquired using the CUSP system (vertical dashed lines in Figures 1h–1k), successfully relocating 101,390 (77%) events. Here we expand this analysis back to 1986 (an extra 67,077 events acquired with the CUSP system) and forward through 2018 (an extra 149,466 events acquired with the AQMS system). This totals 347,445 events representing 32 years of seismicity on the Island of Hawai'i from 1986 to 2018, of which we successfully relocate 275,009 (79%) events. Our resulting catalog is comprehensive in the sense that it represents a complete record of seismicity cataloged by HVO (including automated event triggers) for all of the Island of Hawai'i and its offshore regions. A Gutenberg-Richter (G-R) magnitude-frequency plot (Figure 1f) indicates an approximate (local) magnitude of completion of 1.5, with the caveat that many of the automated event triggers have unassigned magnitudes.

2.2. Waveform Cross-Correlation and Relocation

Our workflow and parameter choices follow those of Matoza et al. (2013). The study by Matoza et al. (2013) introduced a prototype version of the GrowClust relative relocation algorithm, which combines hierarchical cluster analysis and relative relocation with a grid-search L-1 norm method. Waveform cross-correlation is used to improve relative timing accuracy between pairs of seismograms, with correlation-coefficient used as a measure of waveform similarity (e.g., Lin et al., 2007; Waldhauser & Schaff, 2008). Events are sequentially assigned to, and relocated within, similar event clusters in order of pair similarity. Here we use a more recent version of GrowClust by Trugman and Shearer (2017), which incorporates major improvements in the error estimation via bootstrap resampling and additional robustness and quality-control checks.

Waveform data are converted to the custom EFS event-based format, resampled to a uniform 100 Hz sample rate, and filtered 1–10 Hz. Using the starting catalog locations, we pair each event with at least 100 nearest neighbors, or all events within 2 km (~770 million event pairs total). For every such event pair, we perform cross-correlation of P and S phases on all available stations and components. We do not attempt reassociation; we retain the event triggers, waveform windowing, and association as defined by the original starting catalog produced by HVO. We subsequently retain waveform cross-correlation data only for well-correlated (similar event) pairs (defined as pairs with an average P and S waveform correlation-coefficient $r > 0.45$ and at least eight differential time measurements with $r > 0.65$ from source-station distances <80 km). In total, we retain ~1.7 billion high-quality ($r > 0.65$) differential time measurements (P and S)

from ~128 million similar-event pairs. The differential times derived from waveform cross-correlation and the starting hypocenter catalog from HVO are the main inputs to GrowClust.

The calculations were performed on three Linux Symmetrical Multi-Processor/Shared Memory Communication (SMP/SMC) "fat node" high-performance computing (HPC) systems using the slurm workload management system: "tong" 32 × 2.2 GHz Intel CPU cores, 256GB RAM and 8TB local scratch disk; "anvil" 32 × 2.3 GHz Intel CPU cores, 512GB RAM and 11TB scratch; and "forge" 28 × 2.6 GHz Intel CPU cores, 512GB RAM, 7T solid-state drive (SSD) scratch. The cross-correlation computations took several months on these systems, with the best performance achieved with the SSD raid due to I/O (input/output) being a significant limitation in this data-intensive processing.

2.3. Limitations of a 1-D Relative Relocation Approach

As with the work by Matoza et al. (2013), the relocated catalog presented here represents high-precision relative relocation using a 1-D velocity model. Events that group into similar-event clusters are relocated relative to other events within the cluster; however, the absolute location of the cluster centroid remains constrained by the starting catalog hypocenters. Cluster centroids thus retain errors resulting from topography and unknown 3-D velocity structure. A change in the velocity model or unmodeled 3-D velocity structure could rotate the ray parameters, therefore rotating the relative relocations. This should be kept in mind when interpreting our relocations, for example, in terms of the depths, dips, and geometry of inferred seismicity features. The limitations of this 1-D assumption were discussed quantitatively by Matoza et al. (2013) by comparing 1-D relocations with 3-D locations available for a subset of events with analyst phase-pick data (Lin et al., 2014).

Here we aim for comprehensivity in producing high-precision relocations for as much seismicity as possible, providing an advance on the starting catalog produced by routine HVO processing, while acknowledging that a 3-D approach (e.g., Lin et al., 2014) would lead to improvements in absolute location accuracy.

3. Results and Discussion

The relocated seismicity sharpens dramatically (Figures 2 and 3) to reveal features consistent with faults, streaks, rings, rift zones, magma pathways, and mantle fault zones. Our results are generally consistent with previous earthquake relocation studies that have focused on subregions of the island or specific event sequences or types for more limited time ranges (e.g., Battaglia et al., 2003; Gillard et al., 1996; Got & Okubo, 2003; Got et al., 1994; Okubo & Wolfe, 2008; Wolfe et al., 2004, 2003). However, our catalog represents a comprehensive and systematic treatment of all seismicity for the whole Island of Hawai'i spanning multiple decades (1986–2018). Spatiotemporal patterns, including earthquake swarms, "tectonic pulses" (Okubo & Nakata, 2003), and progressive propagation of seismicity downrift in Kīlauea's upper rift zones are apparent in animations of daily seismicity included in the Supporting Information.

On a regional island-wide scale (Figures 2c and 2e), there is a prominent linear seismicity feature at approximately 10 km depth in the Kealakekua region west of Mauna Loa previously interpreted as a basal detachment (Wolfe et al., 2004), broad halos of seismicity surrounding Mauna Kea (Wolfe et al., 2004) and possibly Hualālai volcanoes, and pulses of seismicity at Lō'ihi seamount (e.g., Caplan-Auerbach & Duennebier, 2001), but the bulk of seismicity is concentrated around the active Mauna Loa and Kīlauea and their mobile flanks (Figures 2d and 2f).

In total, we successfully relocate 79% of events across the island, but the percentage of successfully relocated events varies spatially with the density of the starting catalog seismicity. For example, approximately 30% of seismicity around Mauna Kea is successfully relocated, reflecting the relatively sparse seismicity in this region, with fewer events sufficiently well-correlated with nearby seismicity (Figure 2).

3.1. Crustal Detachments and Mantle Fault Zones

Seismicity delineating crustal detachment faults (décollements) separating volcanic pile and old oceanic crust (e.g., Got & Okubo, 2003; Thurber & Gripp, 1988) on the south and west flanks of Kīlauea and Mauna

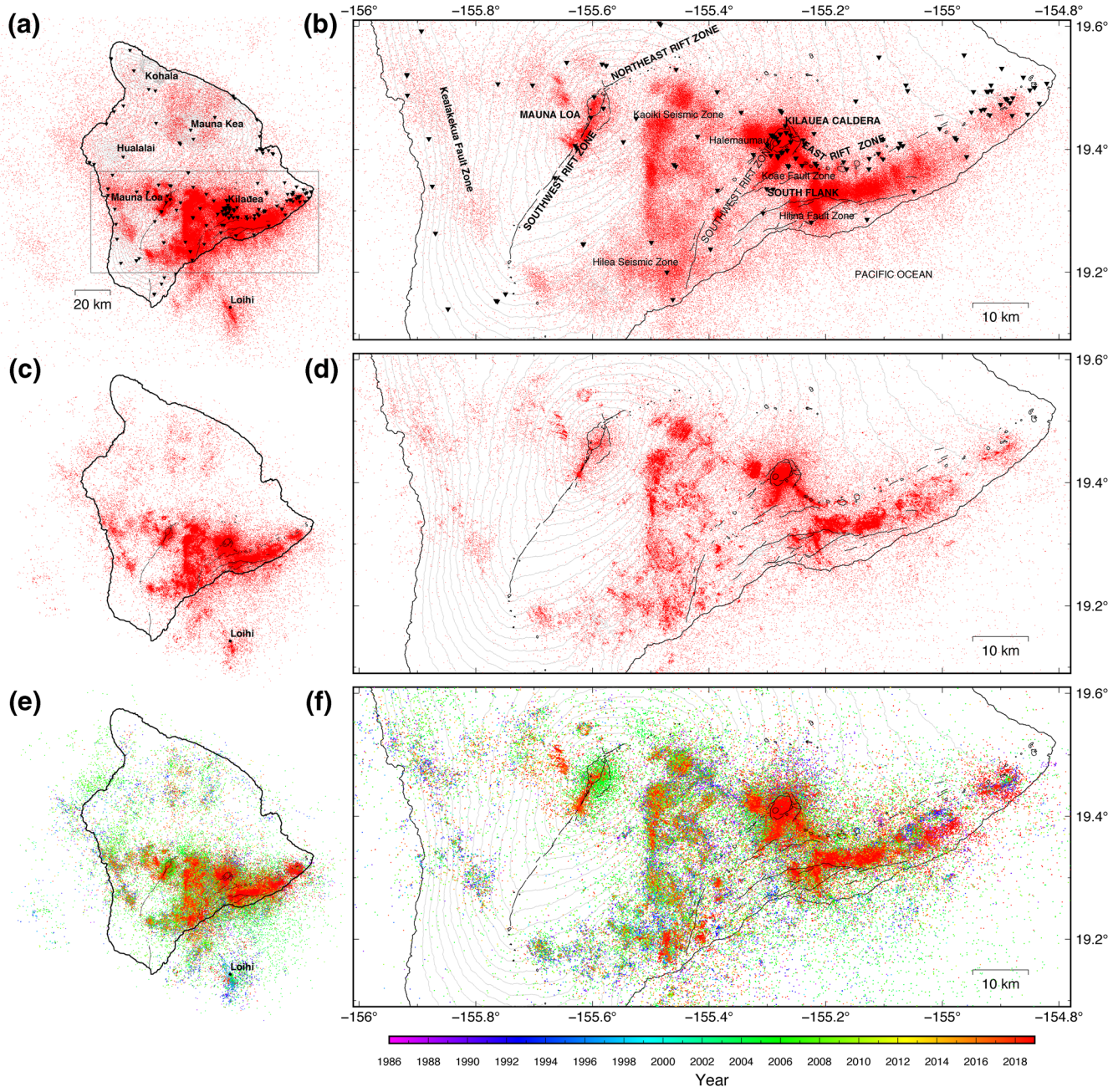

Figure 2. (a and b) The starting catalog and (c and d) our relocated catalog, along with locations of volcanoes (Kīlauea, Mauna Loa, Mauna Kea, Hualālai, Kohala, and Lō'ihi seamount), major faults and seismic zones, and principal morphological features. Black triangles are seismic stations used in this study. Contour interval is 200 m. The box in (a) indicates the region of (b, d, and f). (e and f) The relocated catalog color-coded by time. An animation of this seismicity is included in the Supporting Information. (c–f) show successfully relocated seismicity only (79% of events).

Loa is particularly well-resolved in the relocated catalog (Figure 3). The Kaoiki-Hilea region between Mauna Loa and Kīlauea summits (Figure 3b) is a portion of the detachment with consistently high crustal seismicity rates and where larger earthquakes have occurred (e.g., an *Mw* 6.6 event in 1983). In the Kaoiki-Hilea region (Figure 3b), Mauna Loa's east flank slides southeastward and meets with Kīlauea's southwest flank sliding southward, with motion over the décollement (e.g., Klein et al., 2001; Swanson et al., 1976). The relocations in Figure 3b collapse to a sharp, gently northward dipping plane at ~10 km depth, consistent with a detachment or décollement fault (Got & Okubo, 2003). Numerous compact clusters, streaks, and lineations are prominent in map view (Figure 3b) on this surface. Northward and shallower, we observe parallel lines

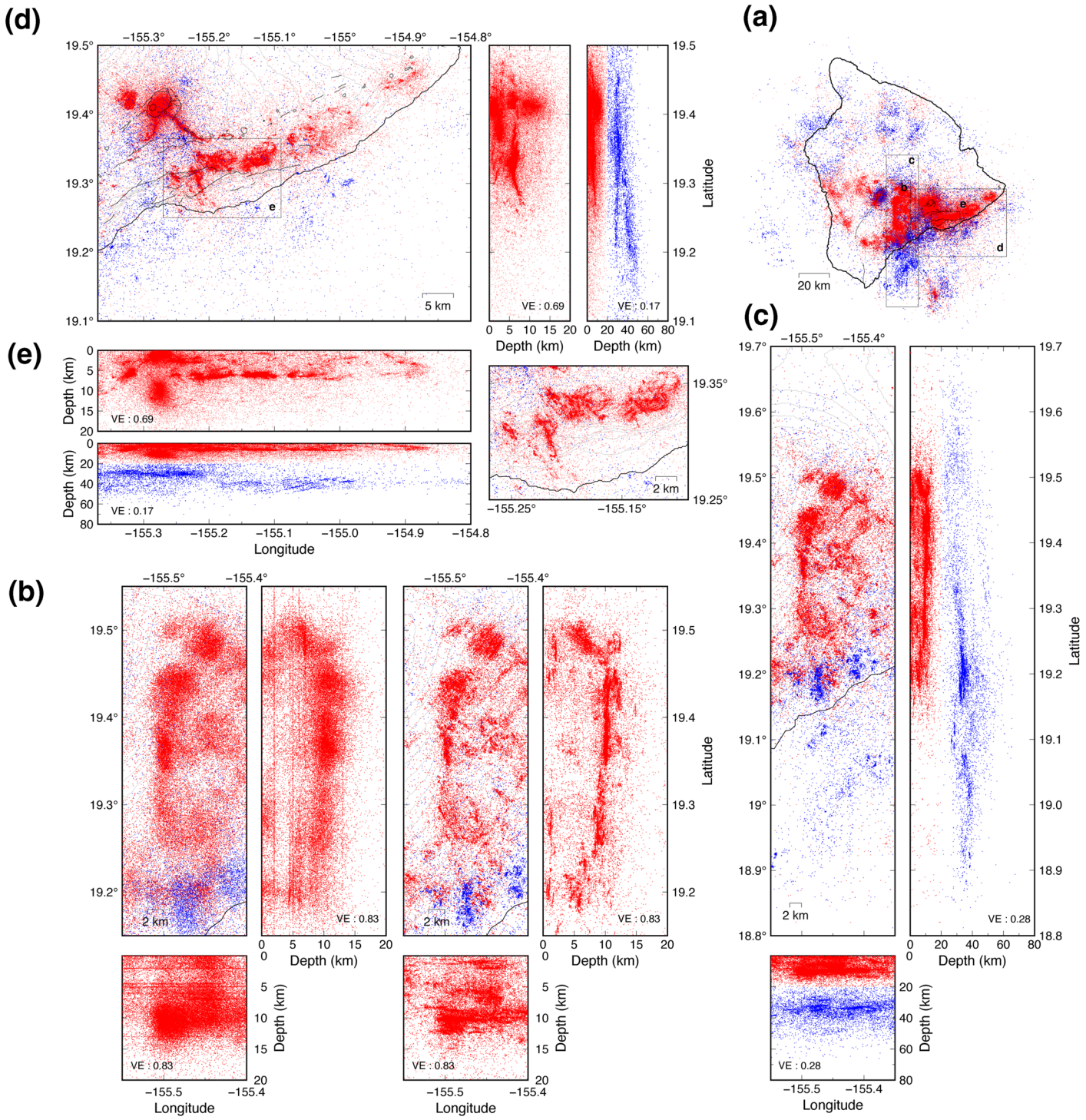

Figure 3. Relocated seismicity on the mobile flanks of Mauna Loa and Kīlauea for 1986–2018; red: events with depths <20 km, blue: events with depths ≥ 20 km. (a) Island of Hawai'i with locations of (b–e). In (b–d), the depth cross-sections only contain events in the accompanying map-view panel latitude and longitude ranges. (b) Seismicity between Mauna Loa and Kīlauea summits, before (left) and after (right) relocation; contour interval is 200 m. (c) View of wider region and expanded depth range (compared to b); contour interval is 200 m. (d) Kīlauea, including its summit, rift zones, and south flank; contour interval is 100 m. (e) Microearthquake streaks on Kīlauea's south flank. VE, vertical exaggeration.

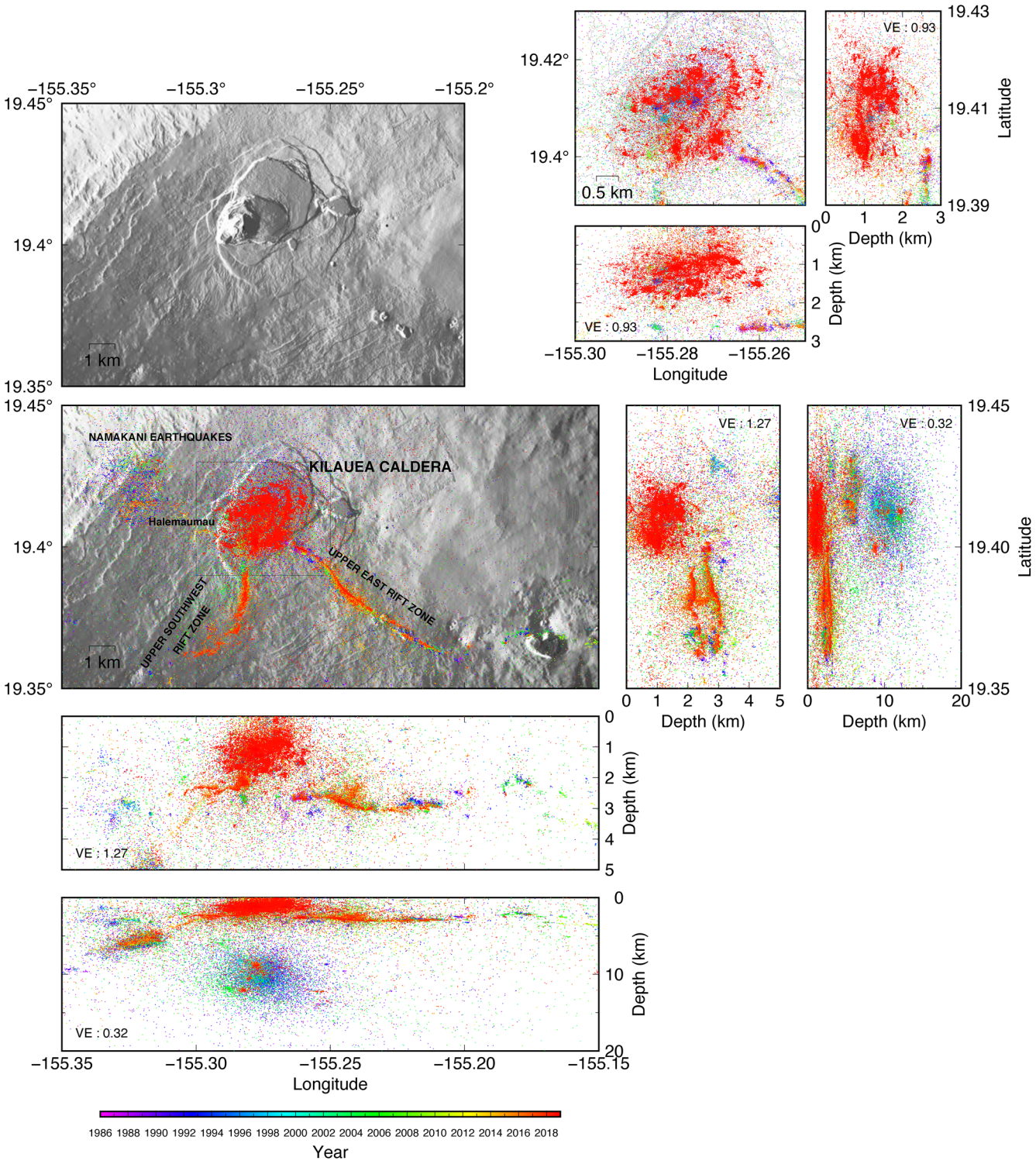

Figure 4. Relocated seismicity 1986–2018 in the Kīlauea summit region. Postsummit-collapse 2018 digital elevation model provided by Ingrid Johanson and Michael Zoeller, Hawaiian Volcano Observatory, US Geological Survey (Mosbrucker et al., 2020). The box in the central panel shows the area of the upper right zoom (contour interval 20 m). An animation of this seismicity is included in the Supporting Information. VE, vertical exaggeration.

of seismicity centered on approximately (−155.445°, 19.485°) previously identified in a smaller data set by Got and Okubo (2003) and interpreted as a zone of strike-slip faults.

Zooming out to a wider region encompassing the Kaoiki-Hilea seismicity and showing seismicity to greater depth (Figure 3c), we observe a laterally continuous diffuse band of seismicity between approximately 20–50 km depth, broadly consistent with a mantle fault zone proposed by Wolfe et al. (2003, 2004), but with tight clustering along a planar feature at approximately latitude 19.2° in Figure 3c.

On Kīlauea's highly mobile south flank, numerous microearthquake streaks (<10 km depth) aligned with geodetic slip (steady creep and slow-slip events) are particularly sharp and prominent features associated with the crustal detachment (Figures 3d and 3e), as observed in previous studies (e.g., Matoza et al., 2013; Rubin et al., 1999; Wolfe et al., 2007). Mantle fault zone features are also visible in the wider region beneath Kīlauea between 20 and 50 km depth (blue dots in Figure 3d).

3.2. Kīlauea Summit and Long-Lived Pu‘u ‘Ō‘ō-Kūpaianaha Eruption

Seismicity in the Kīlauea summit region, including the upper rift zones (Figure 4), represents a complex interplay of tectonic, volcano-tectonic (VT), and long-period seismicity (0.5–5 Hz, LP) (Matoza et al., 2014) and is particularly well-resolved given the dense station coverage in this area (Figure 1e). The Namakani seismic zone (Figure 4) contains sharp earthquake streaks previously identified by Rubin et al. (1999), while bands of seismicity at ∼3 km depth form the seismic expression of the shallow upper Southwest and East Rift Zones (e.g., Gillard et al., 1996; Klein et al., 1987; Okubo & Nakata, 2003; Poland, 2015). Progressive illumination and along-rift migration of the upper rift zone seismicity from 1986 to 2018 is a striking feature of the animations in the Supporting Information.

The long-lived 1983–2018 Pu‘u ‘Ō‘ō-Kūpaianaha eruption of Kīlauea culminated in the 2018 lower East Rift Zone eruption and summit caldera collapse (Neal et al., 2019). At the height of this sequence, cataloged seismicity reaches 24,350 events in the month of July 2018, greatly exceeding typical seismicity rates (Figures 1j and 1k). The 2018 summit seismicity (Figure 4) is largely concentrated at shallow depth <5 km and major relocated features are broadly consistent with those of Shelly and Thelen (2019). Major features include nested arcuate bands of seismicity composed of multiple inward pointing streaks primarily on the east side of the summit collapse area enclosing a nearly complete central seismicity ring and numerous other satellite compact seismicity clusters. Intermediate depth (5–15 km) LP events (Matoza et al., 2014) are part of this seismicity sequence with heightened activity beginning in late 2017. The 2018 lower East Rift Zone and Kīlauea south flank seismicity are also well-captured in the relocation results (Figure 2f).

4. Conclusions

We performed systematic waveform cross-correlation and relative relocation on 347,445 events representing 32 years of seismicity on the Island of Hawai‘i from 1986 to 2018, of which we successfully relocate 275,009 (79%). The resulting relocated catalog provides a sharper image of seismicity features across the Island of Hawai‘i and captures almost the entire 1983–2018 Pu‘u ‘Ō‘ō-Kūpaianaha eruption of Kīlauea. The relocated catalog is available in the Supporting Information.

Data Availability Statement

All data used in this work, including the starting catalog of earthquake hypocenters, phase pick data, and seismic waveform data, are derived from the seismographic network operated by the US Geological Survey (USGS) Hawaiian Volcano Observatory (HVO) and archived at HVO. No new data were used in this work. USGS HVO data are in the US public domain, but not all seismic data used here are currently available via remote database query. Direct contact with HVO personnel is required at present to facilitate data access. Earthquake hypocentral data for earthquakes larger than nominal magnitude M2.0 are accessible from the US Advanced National Seismic System (ANSS) ComCat (https://earthquake.usgs.gov/earthquakes/search/), searchable, for example, using contributor code HV—Hawaiian Volcano Observatory, or via speci-

fication of a geographic search region. Hypocenters of smaller earthquakes, as well as complementary data, including the starting catalog, phase pick data, and seismic waveform data used in this work, are available by contacting HVO (https://volcanoes.usgs.gov/observatories/hvo/; email: askHVO@usgs.gov). Subsets of the data are also available at the IRIS Data Management Center (DMC) (https://ds.iris.edu/ds/nodes/dmc/), seismic network codes HV, PT, IU, NP, PH. Data at the IRIS DMC can be accessed in a variety of ways, for example, by using SeismiQuery (http://www.iris.washington.edu/SeismiQuery/by_network.html) or ObsPy (https://docs.obspy.org/packages/obspy.clients.fdsn.html). The relocated catalog presented in this study is available in the Supporting Information. To produce the starting catalog and extract the data used in this work, all data for located earthquakes occurring from January 1, 1986 through December 31, 2018, with hypocentral coordinates computed using either automatically determined or analyst-reviewed phase arrival times and locating within 150 km of (−155.5°, 19.6°) were extracted from the HVO seismic data archive and converted from native CUSP or AQMS formats into SAC (Seismic Analysis Code) format files, then to the custom EFS format, using programs developed at the University of California, San Diego and University of California, Santa Barbara.

Acknowledgments
This work was supported by NSF grant EAR-1446543. We thank Alicia Hotovec-Ellis for manuscript review. We thank Michael Colee and his team at the Earth Research Institute, University of California, Santa Barbara for maintaining the HPC systems used in this study. We thank HVO and other USGS staff for maintaining the seismic network, thereby enabling studies of long-term seismicity variations.

References

Battaglia, J., Got, J.-L., & Okubo, P. (2003). Location of long-period events below Kilauea Volcano using seismic amplitudes and accurate relative relocation. *Journal of Geophysical Research*, *108*(B12), 2553. https://doi.org/10.1029/2003JB002517

Brooks, B. A., Foster, J. H., Bevis, M. F., Frazer, L. N., Wolfe, C. J., & Behn, M. (2006). Periodic slow earthquakes on the flank of Kilauea volcano,Hawai`i. *Earth and Planetary Science Letters*, *246*, 207–216. https://doi.org/10.1016/j.epsl.2006.03.035

Caplan-Auerbach, J., & Duennebier, F. K. (2001). Seismicity and velocity structure of Loihi Seamount from the 1996 earthquake swarm. *Bulletin of the Seismological Society of America*, *91*(2), 178–190. https://doi.org/10.1785/0119990170

Dawson, P. B., Dietel, C., Chouet, B. A., Honma, K., Ohminato, T., & Okubo, P. (1998). *A digitally telemetered broadband seismic network at Kilauea Volcano, Hawaii* (U.S. Geological Survey Open-File Report, 98–108). https://doi.org/10.3133/ofr98108

Eaton, J. P. (1962). Crustal structure and volcanism in Hawaii. *Geophysical Monograph Series*, *6*, 13–29. https://doi.org/10.1029/GM006p0013

Eaton, J. P., & Murata, K. J. (1960). How volcanoes grow. *Science*, *132*(3432), 925–938. https://doi.org/10.1126/science.132.3432.925

Gillard, D., Rubin, A. M., & Okubo, P. (1996). Highly concentrated seismicity caused by deformation of Kilauea's deep magma system. *Nature*, *384*, 343–346. https://doi.org/10.1038/384343a0

Got, J.-L., Frechet, J., & Klein, F. (1994). Deep fault plane geometry inferred from multiplet relative relocation beneath the south flank of Kilauea. *Journal of Geophysical Research*, *99*(B8), 15375–15386. https://doi.org/10.1029/94JB00577

Got, J.-L., & Okubo, P. G. (2003). New insights into Kilauea's volcano dynamics brought by large-scale relative relocation of microearthquakes. *Journal of Geophysical Research*, *108*, 2337. https://doi.org/10.1029/2002JB002060

Jaggar, T. A. (1920). Seismometric investigations of the Hawaiian lava column. *Bulletin of the Seismological Society of America*, *10*(4), 155–275.

Klein, F. W. (1981). A linear gradient crustal model for south Hawaii. *Bulletin of the Seismological Society of America*, *71*(5), 1503–1510.

Klein, F. W., Frankel, A. D., Mueller, C. S., Wesson, R. L., & Okubo, P. G. (2001). Seismic hazard in Hawaii: High rate of large earthquakes and probabilistic ground-motion maps. *Bulletin of the Seismological Society of America*, *91*(3), 479–498. https://doi.org/10.1785/0120000060

Klein, F. W., Koyanagi, R. Y., Nakata, J., & Tanigawa, W. R. (1987). The seismicity of Kilauea's magma system, volcanism in Hawaii. *U.S. Geological Survey Professional Paper*, *1350*(2), 1019–1185.

Lin, G., Shearer, P. M., & Hauksson, E. (2007). Applying a three-dimensional velocity model, waveform cross correlation, and cluster analysis to locate southern California seismicity from 1981 to 2005. *Journal of Geophysical Research*, *112*, B12309. https://doi.org/10.1029/2007JB004986

Lin, G., Shearer, P. M., Matoza, R. S., Okubo, P. G., & Amelung, F. (2014). Three-dimensional seismic velocity structure of Mauna Loa and Kilauea volcanoes in Hawaii from local seismic tomography. *Journal of Geophysical Research*, *119*, 4377–4392. https://doi.org/10.1002/2013JB010820

Matoza, R. S., Shearer, P. M., Lin, G., Wolfe, C. J., & Okubo, P. G. (2013). Systematic relocation of seismicity on Hawaii Island from 1992 to 2009 using waveform cross correlation and cluster analysis. *Journal of Geophysical Research: Solid Earth*, *118*. https://doi.org/10.1002/jgrb.50189

Matoza, R. S., Shearer, P. M., & Okubo, P. G. (2014). High-precision relocation of long-period events beneath the summit region of Kilauea Volcano, Hawaii, from 1986 to 2009. *Geophysical Research Letters*, *41*. https://doi.org/10.1002/2014GL059819

Mosbrucker, A. R., Zoeller, M. H., & Ramsey, D. W. (2020). *Digital elevation model of Kīlauea Volcano, Hawai'i, based on July 2019 airborne Lidar surveys*: U.S. Geological Survey. https://doi.org/10.5066/P9F1ZU8O

Nakata, J. S., & Okubo, P. G. (2010). *Hawaiian Volcano Observatory seismic data, January to March 2009* (USGS Open-File Report 2010–1079): U.S. Geological Survey.

Neal, C. A., et al. (2019). The 2018 rift eruption and summit collapse of Kīlauea Volcano. *Science*, *363*(6425), 367–374. https://doi.org/10.1126/science.aav7046

Okubo, P. G., & Nakata, J. S. (2003). Tectonic pulses during Kilauea's current long-term eruption. In C. Heliker, D. A. Swanson, & T. J. Takahashi (Eds.), The Pu`u O`o-Kupaianaha eruption of Kilauea Volcano,Hawai`i: The first 20 years (Chap. 11, pp. 173–186): U.S. Geological Survey Professional Paper 1676.

Okubo, P. G., & Wolfe, C. J. (2008). Swarms of similar long-period earthquakes in the mantle beneath Mauna Loa Volcano. *Journal of Volcanology and Geothermal Research*, *178*, 787–794. https://doi.org/10.1016/j.jvolgeores.2008.09.007

Owen, S., Segall, P., Freymueller, J., Miklius, A., Denlinger, R., Árnodóttir, T., et al. (1995). Rapid deformation of the south flank of Kilauea volcano, Hawaii. *Science*, *267* (5202), 1328–1332. https://www.jstor.org/stable/2885996

Poland, M. P. (2015). "Points requiring elucidation" about Hawaiian volcanism. In R. Carey, V. Cayol, M. Poland, & D. Weis (Eds.), Hawaiian volcanoes: From source to surface (Geophysical Monograph Series, Chap. 24, pp. 533–562). https://doi.org/10.1002/9781118872079.ch24

Rubin, A. M., Gillard, D., & Got, J.-L. (1999). Streaks of microearthquakes along creeping faults. *Nature*, *400*, 635–641. https://doi.org/10.1038/23196

Ryan, M. P. (1988). The mechanics and three-dimensional internal structure of active magmatic systems: Kilauea Volcano, Hawaii. *Journal of Geophysical Research*, *93*(B5), 4213–4248. https://doi.org/10.1029/JB093iB05p04213

Segall, P., Desmarais, E. K., Shelly, D., Miklius, A., & Cervelli, P. (2006). Earthquakes triggered by silent slip events on Kilauea volcano, Hawaii. *Nature*, *442*, 71–74. https://doi.org/10.1038/nature04938

Shearer, P., Hauksson, E., & Lin, G. (2005). Southern California hypocenter relocation with waveform cross-correlation, part 2: Results using source-specific station terms and cluster analysis. *Bulletin of the Seismological Society of America*, *95*(3), 904–915. https://doi.org/10.1785/0120040168

Shelly, D. R., & Thelen, W. A. (2019). Anatomy of a caldera collapse: Kīlauea 2018 summit seismicity sequence in high resolution. *Geophysical Research Letters*, *46*, 14395–14403. https://doi.org/10.1029/2019GL085636

Swanson, D. A., Duffield, W. A., & Fiske, R. S. (1976). *Displacement of the south flank of Kilauea Volcano: The result of forceful intrusion of magma into the rift zones* (pp. 1–30): US Geological Survey Professional Paper 963.

Thurber, C. H., & Gripp, A. E. (1988). Flexure and seismicity beneath the south flank of Kilauea volcano and tectonic implications. *Journal of Geophysical Research*, *93*(B5), 4271–4278. https://doi.org/10.1029/JB093iB05p04271

Tilling, R. I., & Dvorak, J. J. (1993). Anatomy of a basaltic volcano. *Nature*, *363*, 125–133. https://doi.org/10.1038/363125a0

Trugman, D. T., & Shearer, P. M. (2017). GrowClust: A hierarchical clustering algorithm for relative earthquake relocation, with application to the Spanish Springs and Sheldon, Nevada, earthquake sequences. *Seismological Research Letters*, *88*(2A), 379–391. https://doi.org/10.1785/0220160188

Waldhauser, F., & Ellsworth, W. L. (2000). A double-difference earthquake location algorithm: Method and application to the Northern Hayward Fault, California. *Bulletin of the Seismological Society of America*, *90*(6), 1353–1368. https://doi.org/10.1785/0120000006

Waldhauser, F., & Schaff, D. P. (2008). Large-scale relocation of two decades of Northern California seismicity using cross-correlation and double-difference methods. *Journal of Geophysical Research*, *113*, B08311. https://doi.org/10.1029/2007JB005479

Wolfe, C. J., Brooks, B. A., Foster, J. H., & Okubo, P. G. (2007). Microearthquake streaks and seismicity triggered by slow earthquakes on the mobile south flank of Kilauea volcano, Hawaii. *Geophysical Research Letters*, *34*, L23306. https://doi.org/10.1029/2007GL031625

Wolfe, C. J., Okubo, P. G., Ekström, G., Nettles, M., & Shearer, P. M. (2004). Characteristics of deep (≥13 km) Hawaiian earthquakes and Hawaiian earthquakes west of 155.55°W. *Geochemistry, Geophysics, Geosystems*, *5*, Q04006. https://doi.org/10.1029/2003GC000618

Wolfe, C. J., Okubo, P. G., & Shearer, P. M. (2003). Mantle fault zone beneath Kilauea volcano, Hawaii. *Science*, *300*(5618), 478–480. https://doi.org/10.1126/science.1082205

Yamada, T., Okubo, P. G., & Wolfe, C. J. (2010). The 2006 Kiholo Bay, Hawaii, earthquake sequence: Relationship of the main shock slip with locations and source parameters of aftershocks. *Journal of Geophysical Research*, *115*, B08304. https://doi.org/10.1029/2009JB006657